Photodissociation Dynamics of Methanol at 157 nm

S. Harich,[†,‡] J. J. Lin,[†] Y. T. Lee,[†,§] and X. Yang*[,†]

Institute of Atomic and Molecular Sciences, Academia Sinica, Taipei, Taiwan, Republic of China, Department of Chemistry, University of California at Santa Barbara, Santa Barbara, California, and Department of Chemistry, National Taiwan University, Taipei, Taiwan, Republic of China

Received: June 16, 1999; In Final Form: September 7, 1999

Photofragment time-of-flight (TOF) spectra at $m/e = 1$(H), 2(H_2, D), 3(HD), and 4(D_2) have been measured for CH_3OH, CH_3OD, and CD_3OH at 157 nm excitation. TOF spectra for photofragments at $m/e = 12$, 13, 14, 15, 29, 30 from the photodissociation of CH_3OH at 157 nm were also obtained. Analysis of these experimental results reveals three different atomic H loss processes: one type of direct hydroxyl H elimination and two types of methyl H elimination. Experimental results also indicate that two molecular hydrogen elimination channels are present: 3-center elimination from the methyl group, which displays two different micro-pathways, and 4-center elimination involving hydrogen atoms on both the C and O sites. The relative branching of the atomic versus molecular hydrogen elimination channels was found to be 1:0.21, indicating that the atomic hydrogen process is still much more significant than the molecular hydrogen process. The C−O bond cleavage channel was also experimentally observed. These results present a uniquely clear picture of methanol photodissociation at 157 nm and thus provide an excellent case for quantitative theoretical investigations.

1. Introduction

Photofragment translational spectroscopy (PTS) in its various forms has been a powerful tool in understanding the dynamics of photodissociation.[1,2] The VUV photolysis of smaller organic molecules often results in several different dissociation processes that lead to similar end products, namely, H and H_2. Separating and understanding the dynamics of such processes is both challenging and interesting. Such systems are theoretically tractable, which allows details of the excited states and fragmentation channels to be calculated with some degree of accuracy.[3−9,14] Between these two sources of information, the complex mechanisms of highly excited molecules can be explored and hopefully understood. Detection of H and H_2 photoproducts using electron impact ionization can be challenging due to high background in the detector and low ionization efficiencies of the fast moving species. Often in PTS experiments information about the H and H_2 dissociation channels comes from the detection of the corresponding heavy fragment, but such measurements can be compromised due to lack of resolution within the experiment and dissociative ionization of the detected fragments in the ionization process. Detection of the H atom has been revolutionized by "Rydberg tagging" techniques.[10] This technique is both precise and sensitive, but, for the dissociation of hydrocarbons where several products are possible, one would like to compare the relative contribution of the various channels to attain a global picture of the dissociation event. Typically, both statistical and dynamic effects are present, and understanding the over all picture of these events would be insightful in understanding the dynamics of highly excited molecules.

The absorption spectrum of methanol in the region of 105−200 nm (Figure 1) has been reported by Nee *et al.*[11] who have assigned (in conjunction with assignments from previous work referenced therein) several features of the spectrum. The long wavelength end of the spectrum shows an absorption continuum 165−198 nm that has been assigned to the 3s ← n Rydberg transition. Progressing toward the shorter wavelength, there are two sharp features at 160 and 150 nm that have been assigned to the different components of the 3p ← n Rydberg transitions. A jet-cooled spectrum with 2.1 Å resolution has been reported[12] in the region of the two 3p transitions (140−160 nm), and with the aid of deuteration the vibrational structure has been assigned to the C−O stretching and CH_3 rocking vibrations. Bersohn and co-workers[13] investigated the photodissociation of methanol at

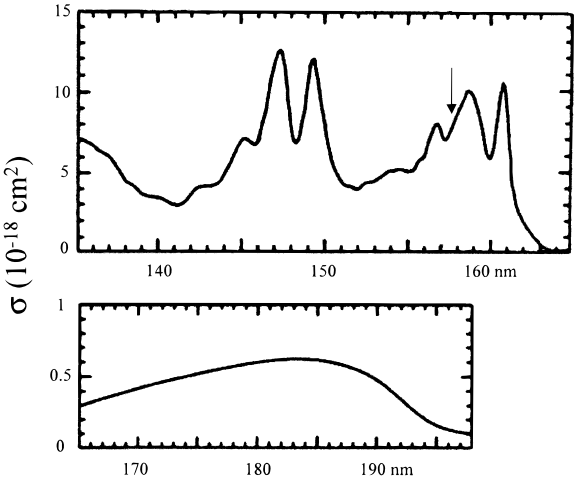

Figure 1. UV absorption spectrum of methanol taken from ref 1. The lower panel shows the absorption spectrum in the 165−198 nm region. The broad continuum in this this panel is attibuted to the 3s ← n transition. The upper panel shows the absorption spectrum in the 135−165 nm region. The spectral features have been assigned to the 3p ← n transitions. The photolysis wavelength (157 nm) in this work is indicated by the arrow.

* To whom correspondence should be addressed. E-mail address: xmyang@po.iams.sinica.edu.tw
† Academia Sinica.
‡ University of California at Santa Barbara.
§ National Taiwan University.

10.1021/jp991987y CCC: $18.00 © 1999 American Chemical Society
Published on Web 11/10/1999

193 nm excitation and concluded that the majority (0.86 ± 0.1) of the methanol dissociation at 193 nm comes from hydroxyl H atom elimination. Experimental evidence suggested that much of the remaining 0.14 ± 0.1 of the yield should be due to the C−O bond cleavage. Ab initio calculations show that the first excited state (3s Rydberg state) of methanol is purely repulsive in the OH coordinate, thus the dissociation of the hydroxyl H is most likely from direct dissociation on the purely repulsive 3s surface.[14] The C−O bond is also repulsive, but there is a small barrier to dissociation that hinders propagation through this channel. Wen et al.[15] have studied the H atom dissociation dynamics of 193 nm photodissociation using H atom high n Rydberg TOF techniques. The TOF spectra obtained exhibited vibrational structure (C−O stretching), and the fit to the spectra showed vibrations in the range of $v = 0-5$, with the most probable at $v = 1$. The vibrational state distribution of the product CH_3O radical reflects the direct nature of the dissociation process.

This work reports PTS spectra for methanol and deuterated derivatives photolyzed at 157 nm excitation. The ability to detect H and H_2 along with the other possible photofragment products has given us a quite complete and uniquely clear picture of the methanol dissociation at 157 nm excitation.

2. Experimental Section

Photofragment translational spectra for methanol photodissociation at 157 nm were obtained using a previously described [16] crossed molecular beam apparatus. This machine consists of a source chamber for the molecular beam, a main chamber, and a rotatable detector that can measure TOF spectra of photofragmentation products as a function of lab angle. The detector consisted of an electron impact ionizer, a quadrupole mass filter (Extrel), and a Daly particle detector. The transient signal output from the detector was discriminated and then recorded using a multichannel scalar (EG&G Ortec, Turbo-MCS). A Lambda Physik LPX210I F_2 laser was used to generate 2−4 mJ of light in a circular spot 4.5 mm in diameter. To suppress the H and H_2 background, the ionization region of the detector was maintained at ultrahigh vacuum conditions ($\sim 10^{-12}$ Torr during data collection). This was accomplished by using three turbo molecular pumps that were backed by a fourth turbo pump, cryopumping from an LN_2 cold surface and from a closed cycle He refrigerator cold head. The He refrigerator was able to lower the H_2 background by a factor of ~70.

Two different experimental setups were used to collect TOF spectra of the photofragments. For the heavy fragments, where the beam velocity spread is the major source of experimental error, a high-resolution configuration was used. A molecular beam of methanol seeded in Ne was generated by the expansion of a methanol/Ne mixture through a 0.5 mm diameter pulsed nozzle. The backing pressure behind the pulsed nozzle was about 250 Torr. Typically, the speed ratio of the molecular beam is about 10. The expanded beam was skimmed twice before it was led into the main chamber, where it was intercepted by the 157 nm photolysis laser. The TOF spectra were recorded at lab angles in the range of 10 to 30°. TOF spectra for all of the possible ions produced were recorded with the exception of $m/e = 28$, where the CO background in the detector is significantly higher than the signal.

The detection of light mass products such as atomic and molecular hydrogen is usually more difficult, and thus a different experimental configuration (low resolution type) was used. In this configuration (which has been used in similar experimental setups[17]), the pulsed valve in the source chamber is perpendicular to the detection direction. A sample of 50 Torr neat methanol (CH_3OH, CD_3OH, CH_3OD, or CD_3OD) was expanded through a 0.5 mm diameter nozzle. The unskimmed molecular beam was then interacted with the photolysis laser at a distance of 7−9 mm from the nozzle tip. The backing pressure was controlled using a temperature control bath (~10 °C). The photofragments were led into the main chamber through an aperture on the source chamber wall that is about 2 cm away from the interaction region. These products then traveled through the main chamber and into the detector. This configuration allowed excellent TOF spectra of the H and H_2 products to be taken in a relatively shorter period of time (typically 40 k laser shots at 50 Hz) because of the increased density of the parent molecules in the interaction region. The poor beam resolution and lack of angular information has little effect on the accuracy of the spectra taken due to the extreme nature of the newton diagrams in the atomic and molecular hydrogen processes.

CH_3OH (99.9%) was purchased from Aldrich, CH_3OD (99.5%) was purchased from Jenssen, while CD_3OH (reported 99.5% D) was purchased from Cambridge Isotopes. All compounds were used without purification. To check for purity, mass spectra of the compounds were taken with an RGA in the source chamber. The mass spectra of CD_3OH showed a significant amount of CD_3OD (5−10%). The mass spectra of the other two compounds were consistent with the quoted purities. It is possible for CH_3OD to exchange the D for H with residual H_2O (and other sources of H) on tubing walls of the sample inlet system. To minimize this problem, the gas inlet system was made as short as possible and the system was passivated with CD_3OD for 24 h and flushed several times with inert gas before a fresh sample was used.

The analysis of the laboratory TOF spectra was performed using a forward convolution program, wherein a TOF spectrum could be simulated by interactive adjustment of the kinetic energy probability distribution curves (P(E)) in the center-of-mass (CM) frame until a satisfactory fit could be obtained. The program takes into account the angular divergence of the beam and detector, the spread in beam velocity, and the length of the ionizer. Using this approach, it is easy to simulate two-body dissociation processes. Three-body dissociation processes[2,18] are more difficult to simulate. The approach used here is based on using two sequential two-body dissociations, where one of the dissociations serves as a primary dissociation, after which, one of the fragments undergoes a secondary dissociation. The recoil velocity of the secondary fragment is distributed over the velocity distribution of the primary fragment. The dynamics of three-body dissociation processes in this fashion can be found in the literature.[2] This approach represents one extreme in the possible three-body dissociation processes. The other extreme would be a simultaneous dissociation where all three fragments leave simultaneously.[18] These cases represent two extremes; the dynamics of most systems often lies somewhere in between. For larger molecules, particularly ones lacking symmetry, the sequential type dissociation should be a good approximation.

3. Results

At the photolysis energy (181 kcal/mol) in this work, there are many thermodynamically possible channels, which are summarized in Figure 2. TOF spectra for the various possible atomic and molecular hydrogen photoproducts (H, D, H_2, HD, and D_2) were obtained for the isotopomers CH_3OH, CH_3OD, CD_3OH, and CD_3OD using the low-resolution configuration. The TOF spectra for the heavy fragments ($m/e > 4$ amu) of the CH_3OH photodissociation at 157 nm were obtained using the

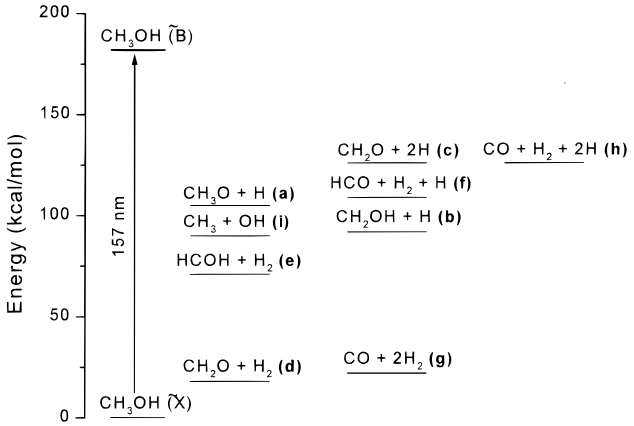

Figure 2. Energy level diagram for the possible products in this experiment. The available energy for a given channel is the difference in height between the photon energy and the channel enthalpy.

high-resolution configuration. In either configuration, great care was taken to ensure the stability of the experimental conditions such that the intensity for the different TOF spectra could be compared somewhat quantitatively. From the experimental TOF spectra, kinetic energy distributions for different channels were obtained. Therefore, detailed dynamics of the methanol dissociation processes can be revealed.

The relative CM flux of the H and H_2 products in the CM frame can be directly extracted from these data. This requires transformation of the laboratory TOF spectra to the CM frame including the beam characteristics, experimental geometry, and ionization cross sections.[19] From these calculations, relative branching ratios can be estimated for different dissociation channels.

Atomic Hydrogen Elimination Processes. TOF spectra at $m/e = 1$ (H) have been measured for the compounds CH_3OH, CH_3OD, and CD_3OH at 157 nm excitation and are shown in Figure 3. Since dissociative ionization of the H_2 product in the detector is very small, the observed $m/e = 1$ signals should all come from the H atom product. Figure 3a shows the $m/e = 1$ (H) TOF spectrum for CD_3OH. The H atom product is clearly from the hydroxyl group of CD_3OH. The observed TOF peak in the spectrum is fast and quite sharp. This is indicative of a direct dissociation on an excited electronic-state surface that correlates with ground-state products, which is very much similar to the methanol photodissociation at 193 nm excitation. The translational energy distribution, P(E) **1** in Figure 4a, was used to fit the observed TOF peak as a single primary two-body process of $H + CD_3O$. The simulated TOF spectrum for this process is shown in Figure 3a and compared with the experimental data. The high energy cutoff of the translational energy distribution obtained is consistent with the available energy for hydroxyl H loss for CD_3OH (process (a) in Figure 2). The translational energy distribution is peaked at quite high energy, indicating that a significant amount of the available energy is partitioned into the translational energy of the photofragments.

Atomic H loss from the methyl group has also been observed in the photodissociation of CH_3OD. Figure 3b shows the TOF spectrum of the $m/e = 1$ product for CH_3OD. There are two distinctive features in this spectrum, one small and fast peak, and one large and broad slow peak. The fast peak can be simulated using P(E) **2** (Figure 4a) translational energy distribution, assuming that these H atom products are resulted from the $H + CH_2OD$ binary dissociation process. The high-energy cutoff of the translational energy distribution obtained is in rather

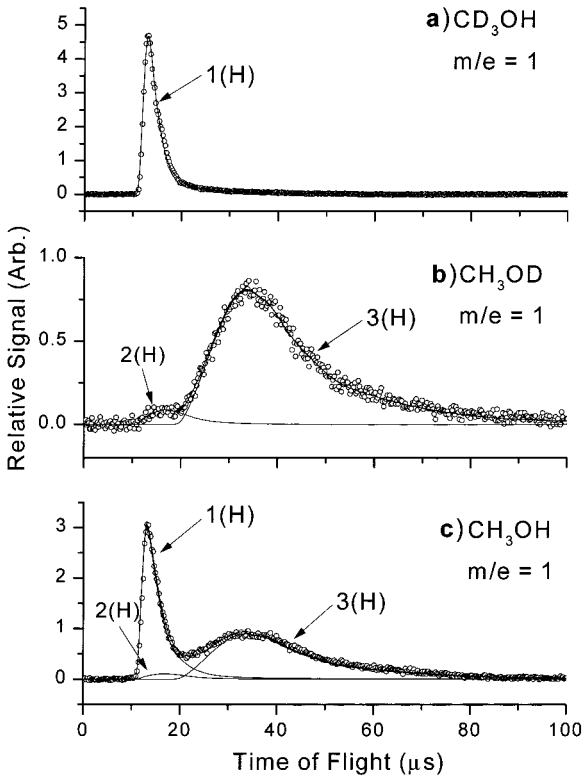

Figure 3. TOF spectra at $m/e = 1$ (H) for (a) CH_3OH, (b) CH_3OD, and (c) CD_3OH. The solid curves fit to the spectra represent signals from different processes and were simulated as two-body dissociation of hydroxyl H (1), two-body dissociation of methyl H (2), and secondary (three-body) dissociation of methyl H (3) from the methoxy radical produced in channel 1. The empty circles represent experimental data, while solid curves are simulated TOF spectra. The neutral product corresponding to each TOF peak is shown in the parentheses. The same convention is also followed in other figures.

good agreement with the available energy for process (b). Therefore, it is not difficult to draw the conclusion that this small fast peak is due to the primary H atom elimination from the methyl group in CH_3OD. The slower broad feature in Figure 3b exhibits a very low product translational energy release (peaked at ~8 kcal/mol).[20] These slow H atom products are obviously coming from the CH_3 group. However, the dynamical sources of these slow H atom products are not immediately clear. From the energy diagram shown in Figure 2, it is quite clear that a significant portion of the CH_3O products from the hydroxyl H atom elimination process should have enough internal energy to further dissociate into $H_2CO + H$ (process (c)). This is clearly a possible source for the slow methyl H atom elimination. A reasonable fit has been obtained for this slow feature in the TOF spectrum using P(E) **1** (Figure 4a) as the kinetic energy distribution of the primary process $CH_3OD \rightarrow (CH_3O)^* + H$, and P(E) **3** (Figure 4b) as the kinetic energy distribution of the secondary dissociation $(CH_3O)^* \rightarrow H_2CO + H$. A nonisotropic CM angular distribution is used in the secondary dissociation, implying that the secondary dissociation should be less than a rotational period. The algorithm used in this simulation can be found in ref 2. The TOF results on the heavy fragments, which will be discussed later, strongly support the above argument that this slower H atom peak in Figure 3b is from the secondary dissociation of the methoxy radical resulting from the primary hydroxyl D (or H) elimination.

From the above investigations of the two deuterated methanol molecules (CD_3OH and CH_3OD), it is quite clear that three types of H atom elimination processes have been identified. These

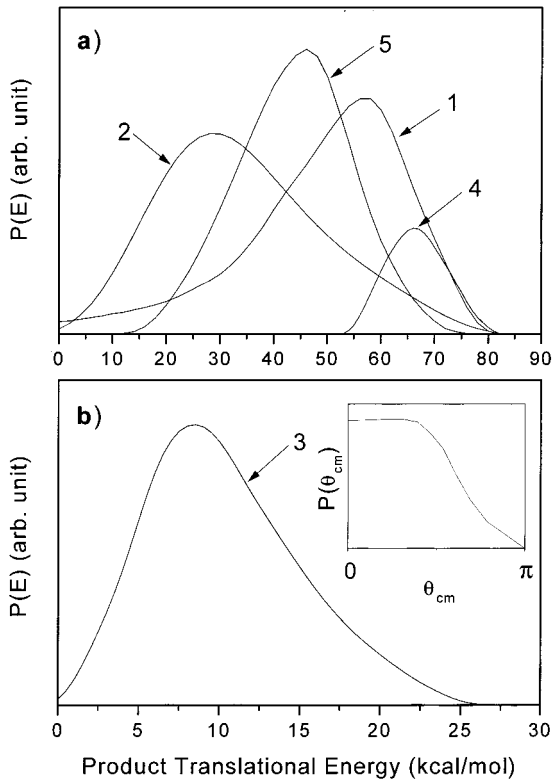

Figure 4. Translational energy distributions used to simulate the various atomic H atom processes. (a) This figure shows the distributions for the hydroxyl H loss from CD_3OH (1), hydroxyl D loss from CD_3OD (5), methoxy radical detected at $m/e = 15$ (4), and two-body methyl H loss (2). (b) This figure shows the translational energy distribution used in modeling the secondary methyl H dissociation (3). The inset on the panel is the CM angular distribution $P(\theta)$ used in the simulation.

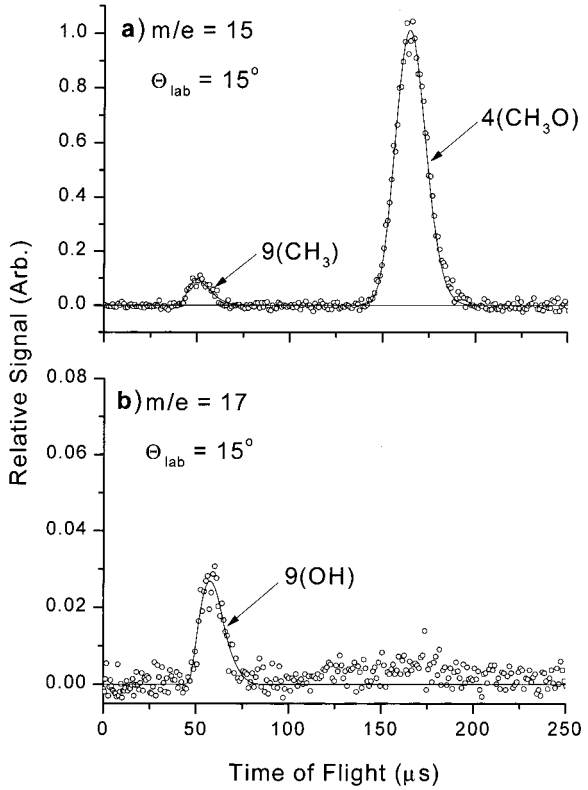

Figure 5. TOF spectra at $m/e = 15$, 17 and $\Theta_{lab} = 15°$ for CH_3OH. The fast peak in both spectra is from the C−O bond cleavage process. The slow peak in (a) is from methoxy radical cracking to CH_3^+. Curve 4 was fit to this peak and should reflect the true two-body process associated with 1 and 3.

three processes can clearly explain the $m/e = 1$ TOF results observed for the CH_3OH molecule. The TOF spectrum for the H atom fragment from CH_3OH at 157 nm is shown in Figure 3c. The spectrum can be simulated using the three H atom elimination processes observed in the deuterated compounds with only minor adjustments in the low energy tail of the P(E) for the hydroxyl atom elimination, and some adjustments of the relative contributions of the three H atom elimination channels. This is quite reasonable since some isotope effects are expected to be present in the photodissociation process. The relative intensities of the atomic processes can also be calculated from this simulation, which gives the following branching ratio for the atomic H loss processes from CH_3OH: Hydroxy H (**1**)/Methyl H (**2**)/Methyl H (**3**) = 1:0.03:0.41.

TOF spectra for heavy radical fragments in the H atom elimination processes have also been measured using the high-resolution configuration setup. However, extensive dissociative ionization of these radical products in the electron impact ionizer could make the interpretation of these results more difficult. For example, the heavy partner of the hydroxyl H atom elimination process from CH_3OH is clearly the methoxy radical. However, detection of the methoxy radical by electron impact ionization is known[21] to be difficult since its parent ion is intrinsically unstable. The methoxy ion will likely crack to HCO^+ predominantly and H_2CO^+ in a small amount.

Let us look at the hydroxyl H atom process first. The methoxy radical partner for this process could appear in the signal at masses 30, 29, 28, 15, 14, 13, and 12. TOF spectra at masses 30, 29, 28 could also have contributions from the other channels such as methyl H loss and H_2 elimination processes. TOF spectrum at $m/e = 15$ (CH_3^+), however, could only have contributions from the primary hydroxyl H loss (a) and the C−O bond cleavage process (i). Figure 5 shows the TOF spectra for $m/e = 15$ and 17 at 20° lab angle. The fast peak in the $m/e = 15$ and $m/e = 17$ TOF spectra clearly corresponds to the C−O bond cleavage channel, which will be discussed later. The slower peak in the $m/e = 15$ TOF spectrum is believed to be from the methoxy radical cracking to CH_3^+. These products should be the primary CH_3O radical products that survived the electron impact ionization process. The translational energy distribution used to fit this slower peak as the $H + CH_3O$ process is shown by P(E) 4 in Figure 4a. The high energy side of this distribution (P(E) 4) overlaps well with that of the translational energy obtained from the hydroxyl H atom product, implying that this is due to the methoxy radical products from the primary hydroxyl H elimination. The low energy side of the distribution (P(E) 4) is, however, completely different from that of the translational energy distribution (P(E) 1) obtained from the primary hydroxyl H atom TOF data. It seems that the lower translational energy part of the CH_3O products, which corresponds to the internally hot CH_3O radicals, is completely missing below 53 kcal/mol. Since the secondary dissociation channel $H + H_2CO$ from CH_3O has an available energy of about 56 kcal/mol, the results shown above clearly indicate that the internally hot CH_3O radical products indeed go though a secondary dissociation process. The H atom product generated from this secondary process should be quite slow as we have observed from the slow H atom products from photodissociation of CH_3OD and CH_3OH. The energy limit (~53 kcal/mol) below which all CH_3O radicals are missing is quite close to the total available energy 56 kcal/mol. This implies that the secondary dissociation process should have a very small barrier if there is one. It is also interesting to point out that the cutoff of the lower

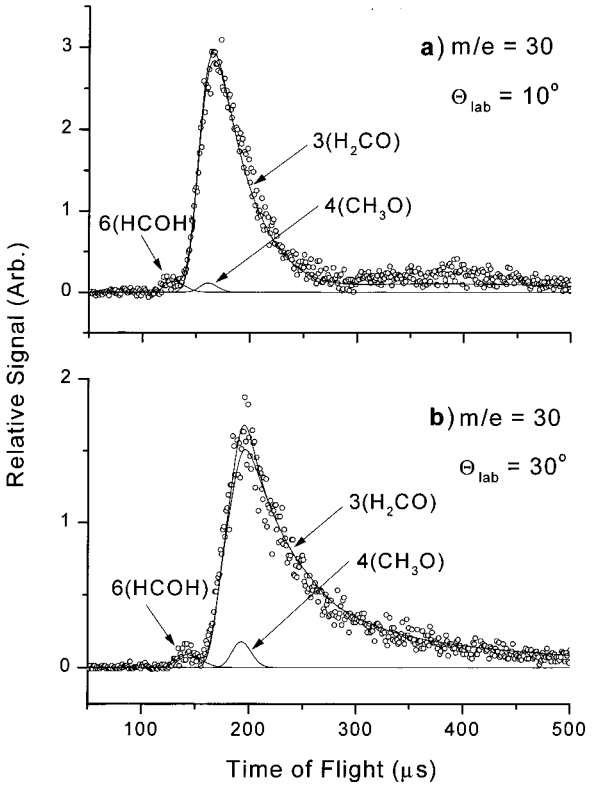

Figure 6. TOF spectra at $m/e = 30$ and $\Theta_{lab} = 10°$ and 30° for CH_3OH. The majority of the signal at this mass comes form the three-body dissociation process (c). The small peak in front is from the fast three-center H_2 elimination process resulting in HCOH (6). Also included in the fit is a small amount of curve 4, which comes from methoxy radical cracking to this mass.

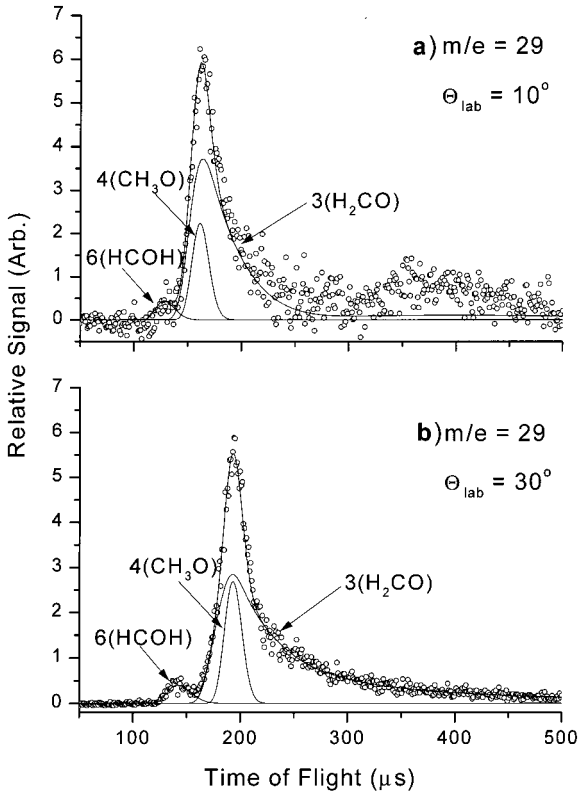

Figure 7. TOF spectra at $m/e = 29$ and $\Theta_{lab} = 10°$ and 30°. The processes used to fit the spectra correspond to the heavy fragment produced in processes 3 and 4. Also, the HCOH fragment produced by the fast three-center H_2 elimination process (P(E) 4) can be seen in front of the main peak.

energy side of the translational energy distribution P(E) 4 (Figure 4a) is not a sharp falloff. This is likely due to the severe dissociative ionization of the internally hot methoxy radical products in the ionizer.

The TOF spectrum (Figure 6) at mass 30 from the CH_3OH photodissociation can also be reasonably fit by including the binary hydroxyl H atom dissociation and the subsequent secondary methyl H loss from the methoxy radical product. In addition, the small peak in front of the TOF spectrum can be attributed to the fast three-center elimination process, which will be discussed in detail in the next section. The $m/e = 29$ TOF spectrum (Figure 7) from the methanol photodissociation can also be explained with the same processes present in the $m/e = 30$ TOF spectrum. However, the relative contributions of these processes to the $m/e = 29$ signal are quite different from those of the $m/e = 30$ signals. The contribution from the binary dissociation process $H + CH_3O$ is significantly enhanced at $m/e = 29$. This is quite reasonable considering the fact that methoxy radical predominately cracks to this mass.

Based on the above investigations of TOF results at both light and heavy masses, the dynamical and site sources of the three atomic H loss processes are clearly identified. The fast hydrogen loss from the hydroxyl group is clearly a direct dissociation on the electronically excited surface. The small H atom elimination from the CH_3 group of methanol is also a binary dissociation, while the slow hydrogen products originated from the CH_3 group are attributed to the secondary dissociation of the internally hot methoxy radical products from the binary hydroxyl H atom elimination process. There are also other possible triple dissociation processes after the H atom elimination from the CH_3 group of methanol. Since this is relatively a very small channel, observation of these triple dissociation channels will not be easy. And certainly their contributions should be quite minor.

Photodissociation of CD_3OD at 157 nm has also been studied in order to check some isotope effects. The TOF spectrum at mass 2 for CD_3OD was measured and is shown in Figure 8a. The spectrum at mass 2 for CD_3OD was very similar to that at mass 1 for CH_3OH. This TOF spectrum can be fitted satisfactorily using the translational energy distributions for the normal methanol molecule with some small adjustments. The methyl D loss process from CD_3OD did not show any significant isotope effect and was fitted using the identical distributions for CH_3OH. The peak of the translational energy distribution (P(E) 5 in Figure 4a) for the D atom loss from the OD group of CD_3OD is, however, shifted toward lower energy by ~10 kcal/mol in comparison to the corresponding process for CH_3OH. This implies that the isotope effect on the hydroxyl H atom elimination process is quite significant. This effect can also be seen in the $m/e = 2$ TOF spectrum from CH_3OD photodissociation (Figure 9a). The TOF spectrum was fitted using the following three channels: one hydroxyl D elimination and two three-center H_2 eliminations. The front peak is attributed to the three-center H_2 elimination process, which will be discussed later. To fit the rest of the peak with hydroxyl D loss, P(E) 5 (Figure 4a) was needed. It is known that the commercial CD_3OH compound is over deuterated by 5−10% as measured by mass spectrometry, and this contamination can be seen in the $m/e = 2$ TOF spectrum (Figure 9b) where D atom loss (curve 7) from the CD_3OD contaminant is observed. The other two contributions in this TOF spectrum were simulated using P(E) 2 and 3 (Figure 4) for the D atom elimination from the CD_3 group. The simulation results are very similar to that of CH_3OH.

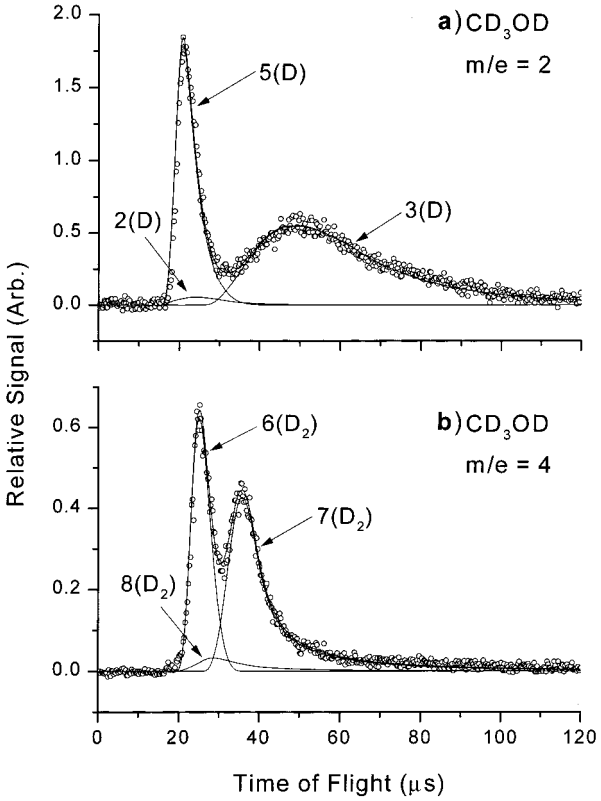

Figure 8. The $m/e = 2$ and 4 TOF spectra for CD_3OD. The distributions used to simulate this spectra were taken from the CH_3OH $m/e = 1$ and 2 data, with the exception of curve 5 which was fit to the spectra in (a). Small adjustments to distributions 6 and 7 were needed to fit the spectra in (b). The adjusted translational energy distributions are all shown in Figure 12 as dashed curves.

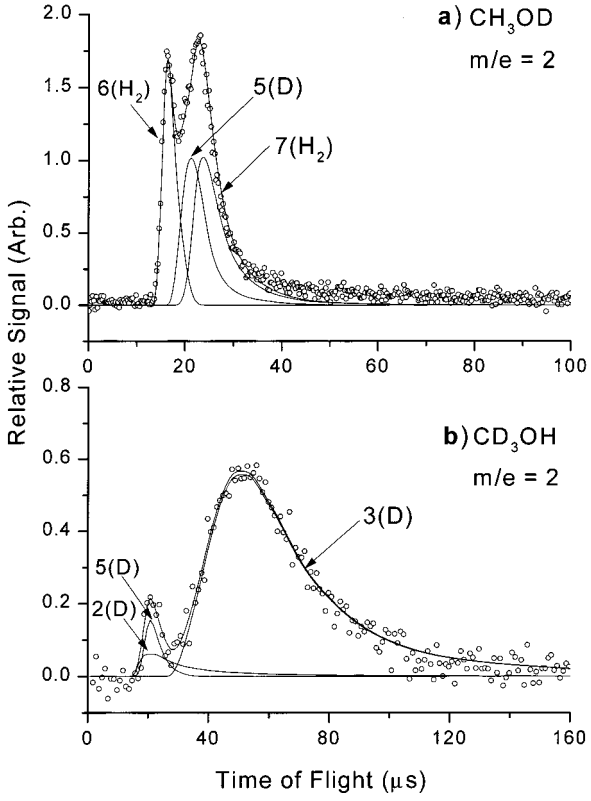

Figure 9. TOF spectra at $m/e = 2$ for CH_3OD and CD_3OH. These TOF spectra contain signals from both atomic and molecular elimination processes. The translational energy distributions used are described in Figures 4 and 12 (see also text). The isotope effect exhibited in curve 5 was needed to fit these spectra.

Molecular Hydrogen Elimination Processes. Molecular hydrogen elimination processes have also been investigated in the photodissociation of methanol at 157 nm. Figure 10b shows the $m/e = 4$ TOF spectrum for CD_3OH. The signal at mass 4 is obviously from the three-center molecular D_2 elimination from CD_3OH exclusively. Two features are clearly observed in the TOF spectrum, indicating that there are two different D_2 elimination processes. These peaks were simulated using two different translational energy distributions as binary D_2 elimination from CD_3OH. The fast peak in the TOF spectrum at $m/e = 4$ is fitted using P(E) 6 (dashed curve) in Figure 12. The high energy cutoff is quite consistent with the available energy for process (e). This distribution is also peaked at relatively high energy, implying that the elimination likely occurs on an excited electronic surface which correlates with the ground-state products. The slower peak can be simulated using P(E) 7 in Figure 12, which is shifted to somewhat lower energy. This slower peak is due to either a dissociation pathway that produces an electronically excited HCOH product or a triple dissociation process. Further identification is not possible at the moment.

The $m/e = 3$ TOF spectra for the molecules CH_3OD and CD_3OH are shown in Figure 11 (a and b, respectively). The signals in these TOF spectra could only come from a four-center HD elimination process. These TOF spectra are significantly different from that of the three-center elimination process (Figure 10a, b). The two TOF spectra (Figure 10a, b) at mass 3 can be fitted using two very similar translational energy distributions shown in Figure 12 (P(E) 8 solid and dashed lines, respectively). It is clear that the translational energy distribution P(E) 8 extends beyond the available energy for process (e) and approaches the available energy for process (d). Ab initio calculations[5] on the ground electronic surface for the four-center H_2 elimination process yields an exit barrier of ~92 kcal/mol. With a barrier of this magnitude one would expect to find a kinetic energy distribution at least qualitatively similar to P(E) 8 which is peaked some where in the middle[22] of the available energy with a rather broad overall character. From the above investigations, it is immediately clear that there are at least three distinctive molecular hydrogen elimination processes from methanol photodissociation: two three-center micropathways from the CH_3 group and one four-center elimination process which is much smaller than the three-center processes.

The $m/e = 2$ TOF spectrum for CH_3OH (Figure 10a) was simulated using a combination of the above three processes with some small adjustments. The three-center processes used to simulate this spectrum (P(E) 6 and 7) were adjusted by a small amount in comparison to the distributions obtained from the D_2 elimination processes. In Figure 12 the dashed curves P(E) 6 and 7 are the translational energy distributions obtained from the D_2 processes, while the solid curves P(E) 6 and 7 were used to fit the H_2 TOF spectrum from CH_3OH. The branching ratios for the methanol molecular hydrogen elimination processes were determined to be fast 3-c (P(E) 6)/slow 3-c (P(E) 7)/4-c (P(E) 8) = 1:0.87:0.11. The relative branching ratio for the atomic and molecular hydrogen processes from methanol photodissociation has also been determined to be atomic hydrogen/molecular hydrogen = 1:0.21.

Molecular hydrogen processes have also been studied in the photodissociation of CD_3OD and CH_3OH. The TOF spectrum at mass 4 from CD_3OD is shown in Figure 8a, while the TOF spectrum at mass 2 from CH_3OD photodissociation is shown in Figure 9a. These TOF spectra can be easily simulated using the translational energy distributions P(E) 6, 7, and 8 for the

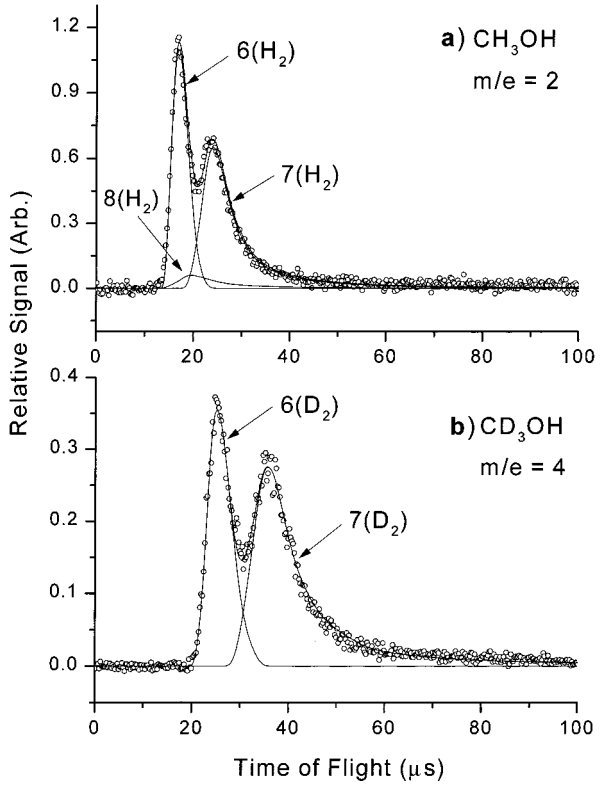

Figure 10. TOF spectra for the three-center molecular hydrogen loss channels: (a) CD_3OH $m/e = 4$ and (b) CH_3OH $m/e = 2$. Curves 6 and 7 are the simulated three-center elimination processes, while curve 8 is the four-center elimination process. Curves 6 and 7 needed to be adjusted by a small amount to fit the spectra in (a) and (b). Curves 6 and 7 in Figure 12 are displayed as solid and dashed curves to show the differences needed to fit the H_2 vs D_2 elimination, respectively.

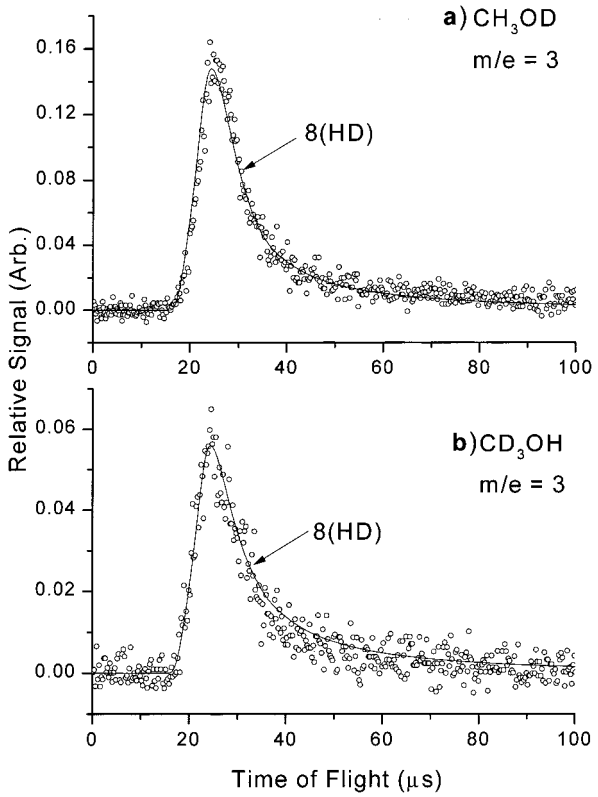

Figure 11. TOF spectra for the four-center molecular hydrogen loss channels: (a) CD_3OH $m/e = 3$ and (b) CH_3OD $m/e = 3$. P(E) 8 (solid and dashed curves in Figure 12) were used to fit these two spectra for CH_3OH and CD_3OD, respectively. Minor differences are found between the above four-center processes.

molecular hydrogen elimination process, indicating that the whole picture presented above is quite consistent. Due to the small contribution from the H_2 elimination processes relative to the atomic H channels, the heavy radical fragments from most of the H_2 elimination channels are normally difficult to identify. The only identifiable molecular hydrogen channel in the heavy product TOF spectra is the three-center elimination process (P(E) 6) seen as a small fast peak in the TOF spectra at $m/e = 29$ and 30. Other small H_2 elimination processes should be hidden underneath the large peaks in all the TOF spectra.

C−O Bond Cleavage. As discussed earlier, the C−O bond cleavage channel has also been clearly observed. Figure 5 shows the TOF spectra at $m/e = 15$ and 17. The fast peak in both of these spectra is obviously due to the C−O bond cleavage process. A single translational energy distribution (P(E) 9 in Figure 13) is used to fit both features at mass 15 and 17 as a binary $CH_3 + OH$ dissociation processes. The energy cutoff of the kinetic energy distribution is consistent with the available energy for this process. The product kinetic energy distribution indicates that quite significant amount of the available energy is partitioned into the product translational degree of freedoms, implying a direct dissociation process for the C−O bond cleavage. Without knowing the relative contribution of the methoxy radical to this TOF spectrum, it would be difficult to determine the relative contribution of the C−O cleavage channel with respect to the other observed channels. But considering the fact that for the $m/e = 15$ TOF spectra the C−O cleavage processes represents ∼60% of the signal in the CM frame, the overall contribution from the C−O cleavage process is certainly not very minor.

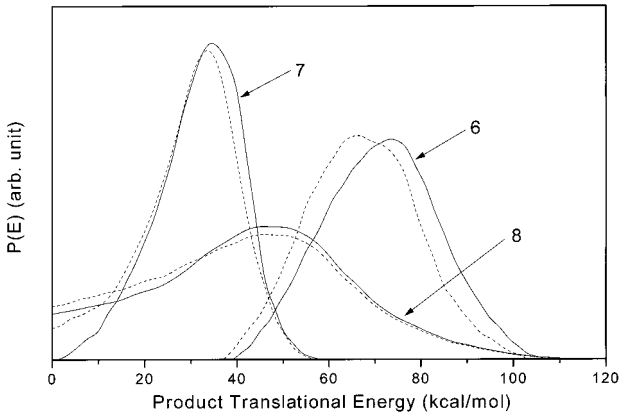

Figure 12. Translational energy distributions for the molecular hydrogen channels. P(E) 6 and 7 are the three-center elimination processes, where the solid curves are from the H_2 elimination processes, and the dashed curves are from the D_2 elimination. P(E) 8 is the four-center elimination process, where the solid curve was from CH_3OD $m/e = 3$ data and the dashed curve was from the CD_3OH $m/e = 3$ TOF data.

4. Discussion

It is clear that the dissociation of methanol on the 3p Rydberg surface is significantly more complex than dissociation on the 3s surface. The topology of the 3p electronic surface has not been studied extensively. Theoretical studies[8,9] that have investigated the 3p state show that the OH bond on the 3p surface is bound. These investigations also show avoided crossings between the 3s and 3p surfaces, which would imply that there are strong couplings between these two surfaces. The vibrational structure (see Figure 1) observed in the absorption

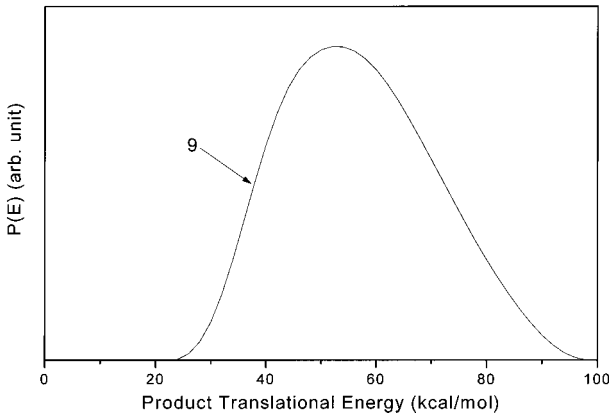

Figure 13. Translational energy distribution for the C−O bond cleavage process (P(E) 9).

spectrum indicates that excited methanol molecules in the 3p state live at least for a short period of time (likely a few vibration periods). This would also imply that at least some degree of energy randomization must also take place. Considering the fact that both the C−O bond and the O−H bond are repulsive on the 3s surface, it seems clear that the system undergoes fast internal conversion to the 3s surface after it is excited to the 3p state, and then dissociates on the 3s surface. The kinetic energy distributions for these processes indicate that a significant amount of energy has been deposited into the product translation. For both C−O and O−H bond rupture processes, quite a large amount of energy is also partitioned into internal coordinates of the fragments. This internal excitation can be seen in the secondary dissociation of the methoxy radical, modeled by P(E) 3. Another interesting experimental result is the fast three-center H_2 elimination process (P(E) 6 in Figure 12). It is clear from the translational energy distribution obtained from the TOF spectra of both fragments (H_2 and HCOH) that the dissociation likely occurs on an excited-state surface that correlates with ground-state products. Typically, H_2 elimination processes have high barriers to dissociation, and thus it is unusual to find an H_2 elimination process that is as direct as this example.

There is some evidence for internal conversion to and dissociation from the ground-state electronic surface. The distribution obtained for the two-body methyl H loss process (P(E) 2 in Figure 4a) shows a process that has a large spread in kinetic energy and is also peaked at low energy. Excited-state dissociation is less likely to produce a distribution of this character. The heavy fragment that would correspond to this process could not be identified due to its small branching ratio. Another process that is likely to occur on the ground electronic surface is the four-center H_2 elimination process. The distribution obtained for this process resembles dissociation over a sizable barrier, peaked somewhere in the middle of the available energy for the process, with a broad distribution overall.

Out of all of the major features of the various spectra shown here, the slow peak in the three-center H_2 elimination process (P(E) 7, Figure 12) is the least understood. One possibility is that this process is part of a three-body dissociation process corresponding to (f). Similar to the secondary methyl H loss discussed above, process (f) should occur to some degree if the internal energy of methoxy radical is high enough to overcome the dissociation barrier. With this in mind, an attempt was made to fit the peak as a secondary H_2 elimination from methoxy radical (P(E) 1, Figure 4a). The distribution obtained from the fit was rather sharp (∼10 kcal/mol fwhm) and centered at ∼36 kcal/mol. However, due to numerical instabilities of simulating a secondary dissociation with energy distributions that are sharp, the simulated TOF spectrum obtained contains large oscillations on the slow end of the TOF spectra. Using this sharp P(E) to fit the $m/e = 29$ TOF spectra at both 10° and 30° lab angle (looking for the HCO that would come from this channel), the broad underlying peak could be simulated satisfactorily, provided that the CM angular P(θ) distribution was also sharp. The sharp angular and energy distributions obtained from this attempted fit are an indication that this secondary process is not a simple sequential process and would require more sophisticated methods to simulate its contribution to the TOF spectra. Whether or not this process is occurring does not change the overall picture developed here. The possible contribution of this process to the $m/e = 29$ TOF spectra does not change the interpretation of the rest of the data because the extent of cracking to this mass from the H_2CO product is unknown. This means that for the $m/e = 29$ TOF spectra the contribution from the proposed channel could be mixed with an arbitrary amount of the identified processes, and an equally good fit could be obtained. This slow three-center molecular hydrogen process could also be due to the electronically excited HCOH radical products. In any case, further modeling and experiments are needed in order to clarify this slow three-center molecular hydrogen elimination process.

5. Conclusion

The 157 nm photodissociation of methanol has been investigated using PTS techniques. H and H_2 were detected directly using a "universal" detector with extremely low background at these masses. Simulation of the photofragment TOF spectra reveals several dissociation pathways for the atomic and molecular hydrogen loss channels. The hydroxyl H undergoes fast conversion from the B (3p) surface to the repulsive A (3s) surface. This process partitions most of the available energy into the product translational degrees of freedom. A significant amount of energy is also partitioned into internal degrees of freedom of the radical products. The methyl H atom loss occurs in two major pathways. First is a secondary H loss that comes from the highly excited methoxy radical produced by the hydroxyl H loss pathway. The other methyl loss channel is a primary process that has a broad distribution of energy. Three distinctive H_2 elimination processes were also observed, two of which correspond to three-center elimination from the methyl group, while the other one corresponds to four-center elimination.

Acknowledgment. We are very pleased to make this contribution to this special issue of Journal of Physical Chemistry in honor of Professor Kent R. Wilson who has made tremendous contribution to this research field. This work is supported by the National Science Council and the Academia Sinica of the Republic of China. Financial Support from the China Petroleum Co. is also gratefully acknowledged.

References and Notes

(1) Wodtke, A. M.; Lee, Y. T. In *Advances in Gas-Phase Photochemistry and Kinetics;* Royal Society of Chemistry: London, 1987.
(2) Zhao, X. Ph.D. Thesis, University of California, 1988.
(3) Curtiss, L. A.; Kock, D. L.; Pople, J. A. *J. Chem. Phys.* **1991**, *95*, 4040.
(4) Bauschlicher, C. W., Jr.; Langhoff, S. R.; Walch, S. P. *J. Chem. Phys.* **1992**, *96*, 450.
(5) Walsh, S. P. *J. Chem. Phys.* **1993**, *98*, 3163.
(6) Cui, Q.; Morokuma, K. *Chem. Phys. Lett.* **1996**, *263*, 54.
(7) Deng, L.; Ziegler T.; Fan, L. *J. Chem. Phys.* **1993**, *99*, 3823.
(8) Buenker R. J.; Olbrich, G.; Schuchmann, H.-P.; Schurmann, B. L.; von Sonntag, C. *J. Am. Chem. Soc.* **1984**, *106*, 4362.
(9) Larrrieu, C.; Chaillet, M. *Nouv. J. Chim.* **1981**, *5*, 365.

(10) Schnieder, L.; Meier, W.; Welge, K. H.; Ashfold, M. N. R.; Western, C. M. *J. Chem. Phys*. **1990**, *92*, 7027.
(11) Nee, J. B.; Suto, M.; Lee, L. C. *Chem. Phys.* **1985**, *98*, 147.
(12) Sominska, E.; Gedanken, A. *J. Mol. Spectrosc.* **1996**, *175*, 234.
(13) Satyapal, S.; Park, J.; Bersohn, R. *J. Chem. Phys*. **1989**, *91*, 6873.
(14) Marston, C. C.; Weide, K.; Schinke, R.; Suter, H. U. *J. Chem. Phys.* **1993**, *98*, 4718.
(15) Wen, Y.; Segall, J.; Dulligan, M.; Wittig, C. *J. Chem. Phys*. **1994**, *101*, 5665.
(16) Lin, J.; Hwang, D. W.; Harich, S.; Lee, Y. T.; Yang, X. *Rev. Sci. Instrum.* **1998**, *69*, 1642.
(17) Balko, B. A., Ph.D. Thesis, University of California at Berkley, 1991.
(18) Maul C.; Gericke, K.-H. *Int. Rev. Phys. Chem.* **1997**, *16*, 1.
(19) Experimental values for the ionization cross section for H and H_2 at 70 eV have been reported. For H_2 a value of 9.8×10^{-17} cm^2 was obtained from the following references: Saksena, V.; Kushwaha, M. S.; Khare, S. P. *Physica B* **1997**, *233*, 201. Rapp, D.; Englander-Golden, P. *J. Chem. Phys.* **1965**, *43*, 1464. Tate, J. T.; Smith, P. T. *Phys. Rev.* **1932**, *39*, 270. For H atom a value of $7 (\pm 1.5) \times 10^{-17}$ cm^2 was used, which was obtained from the following references: Hu, W.; Fang, D.; Wang, Y.; Yang, F. *Phys. Rev. A* **1994**, *49*, 989. Shyn, T. W. *Phys. Rev. A* **1992**, *45*, 2951. Fite, W. L.; Brookman, R. T. *Phys. Rev.* **1958**, *112*, 1141. Rothe, E. W.; Marion, L. L.; Neynaber, R. H.; Trujillo, S. M. *Phys. Rev.* **1962**, *125*, 582.
(20) Harich, S.; Lin, J. J.; Lee, Y. T.; Yang, X. *J. Chem. Phys.*, in press.
(21) Lin, J. J.; Lee, Y. T.; Yang, X. *J. Chem. Phys.* **1998**, *109*, 2975.
(22) Mordaunt, D. H.; Osborn, D. L.; Neumark, D. M. *J. Chem. Phys.* **1998**, *108*, 2448.